

## A Panchromatic Study of the Gravitational Lens MG J0751+2716 at Redshift 3.2

© C. Spingola, J. P. McKean, M. Rybak, H. R. Stacey,  
S. Vegetti, M. Auger, C. Fassnacht, L. V. E. Koopmans,  
D. Lagattuta

Kapteyn Astronomical Institute, Landleven 12, 9747 AD Groningen, NL

To better understand the connection between AGN and their host galaxies, we performed a detailed multi-wavelength analysis of the gravitationally lensed radio-loud AGN MG J0751+2716 at redshift 3.2. This object consists of extended gravitational arcs and two compact components, which are clearly detected in the HST F555W and F814W filters, Keck AO  $K'$ -band and EVN observations at 1.65 GHz. By carrying out a pixellated reconstruction of the background source, we spatially locate the stellar population of the AGN host galaxy and the radio core and jets. Our source reconstruction finds that the evolved stellar population is more compact with respect to local early-type galaxies, while the blue component extends several hundreds of parsecs and is off-set from the radio jet.

**Keywords:** VLBI, Gravitational Lensing, Active Galactic Nuclei.

### 1 Introduction

The co-evolution between active galactic nuclei (AGN) and their host galaxies, and how strong the connection is between the relativistic jets and star-forming episodes, are still unclear. Understanding exactly how newly formed stars and the central AGN are connected is important especially in galaxies at  $z \sim 2 - 4$ , where the bulk of the stellar population is formed and the AGN peak activity takes place [7]. A powerful tool to study these systems is the analysis of their spectral energy distribution (SED), especially in the infrared and radio wavelength regimes, to determine the relative contribution of star-formation and AGN activity. Star-forming galaxies are rich in dust, and the UV radiation emitted by newly formed stars and possible AGN is generally absorbed by dust and re-emitted in the infrared part of the spectrum. This

leads to an SED that typically has a peak at  $\sim 100 \mu\text{m}$  due to star-formation, and a bump in the mid-infrared part of the SED due to the dust in the torus that is heated directly by the central AGN [9]. Even if the SED features are distinct, the relative importance of star-formation and AGN activity is still uncertain. It is believed that when the AGN is in the *radio mode* of activity, the star-formation may be triggered by radiative shocks as they encounter the clumpy interstellar medium, inducing the collapse of the surrounding molecular clouds [14]. However, the *positive feedback* from AGN alone can not account for the extremely high star-formation rates (SFR) observed in some high redshift galaxies. In fact, galaxy mergers and interactions are likely to be the main cause of starburst activity within primordial galaxies, and they can provide a significant amount of fuel for star-formation [4]. The scales where AGN and star-formation act are small [3, 8] and, therefore, studying the AGN feedback is challenging especially at high redshifts, because of the intrinsic limitations in sensitivity and angular resolution of current instruments. However, if a massive galaxy lies along the line-of-sight, a background source can be magnified and enlarged because of the *gravitational lensing* effect. In this case we obtain a high angular resolution view of its smallest regions that would otherwise be impossible to observe [15, 16]. When observations are coupled with advanced gravitational lens modeling algorithms, it is also possible to recover the intrinsic morphology of the different components in the system [12, 13]. Thereby, the interplay between the AGN and its host galaxy can be inferred on 1–100 pc scales.

## 2 Multi-wavelength imaging of MG J0751+2716

MG J0751+2716 was discovered as part of the MIT-Green Bank survey with the VLA and was later observed with MERLIN at 6 cm, showing four components separated by  $\sim 0.8$  arcsec, some of which form large gravitational arcs [6]. The redshifts of the lensing galaxy and the background source were found to be  $z_L = 0.35$  and  $z_S = 3.2$ , respectively [17]. Moreover, CO molecular gas emission at cm and mm wavelengths was found with the EVLA and GBT, implying a significant gas reservoir and, therefore, possible on-going star-formation [1, 11]. In order to clarify the AGN and star-formation conditions in this high-redshift galaxy, we have analyzed higher angular resolution observations. The available data for this object span the rest-frame UV to radio spectrum, giving an opportunity of investigating all of the components in this system.

### 2.1 Optical / IR observations

The Keck 2.2  $\mu\text{m}$  adaptive optics imaging for MG J0751+2716 were taken as part of the *Strong-lensing at High Angular Resolution Program* (SHARP)

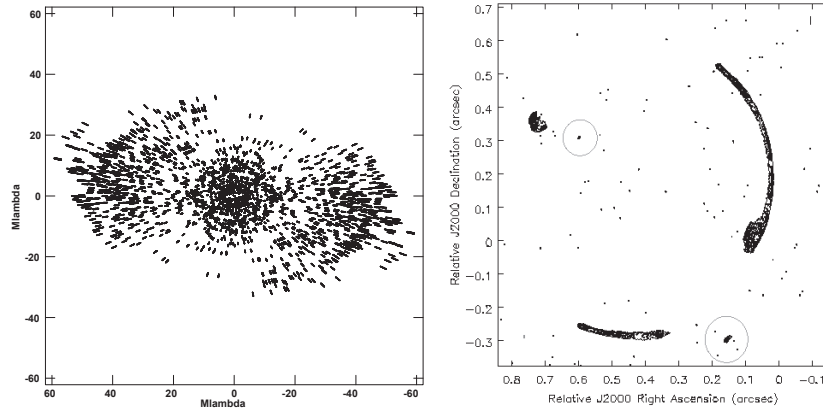


Fig. 1. *Left*:  $uv$ -coverage of GM070 observation for MG J0751+2716 at 1.65 GHz. Only one out of every ten visibilities are plotted. *Right*: Continuum image at 1.65 GHz of MG J0751+2716. The magenta circles highlight the new double component detected by this observation. The peak flux density is  $37 \text{ mJy beam}^{-1}$ . The restored beam is  $2 \times 7 \text{ mas}^2$  in p. a.  $-12.38^\circ$ , plotted in the bottom left corner. The first contour is the off-source noise level measured on the image plane ( $18 \mu\text{Jy beam}^{-1}$ ). Contour levels increase by a factor of 2

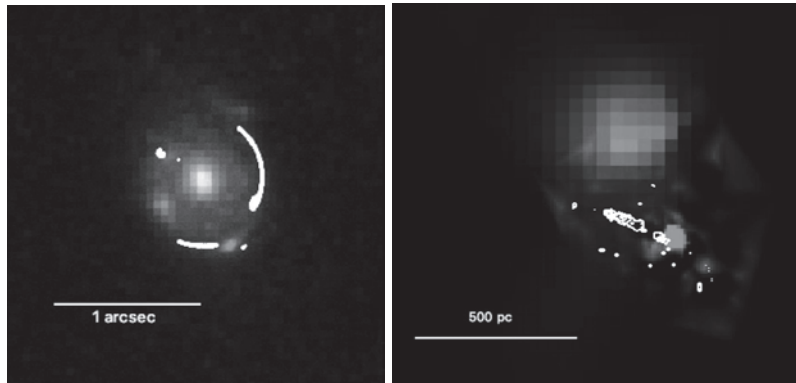


Fig. 2. *Left*: RGB rendering using Keck AO K' filter (compact and diffuse emission almost coincident with the radio contours), HST F555W and F814W (double component offset from the arcs) and EVN at 1.65 GHz (white contours) of the lensed system MG J0751+2716. *Right*: Reconstructed source. The white contours are the radio source, the source reconstruction of the HST observations is the more extended component (at the top) and the more compact component (close to the radio contours) is the reconstructed source from Keck AO data

program [5]. Archival optical observations with the *Hubble Space Telescope* through the F555W and F814W filters were taken using WFPC2. A colour composite image of the optical/infrared imaging is presented in Fig. 2 and shows a compact blue component that is doubly imaged and one extended red component.

## 2.2 Radio observations

MG J0751+2716 was observed with the global VLBI Array on 2012 October 21 (project GM070; PI: McKean). The observation included all of the EVN and the VLBA antennas; Lovell, Effelsberg, Rob70 and GBT were included to increase the sensitivity. The excellent  $uv$ -coverage provided by the global-VLBI observation (Fig. 1) is fundamental for a detailed study of the structure of extended arcs. The observations were carried out at 1.65 GHz with a duration of  $\sim 13$  hours. The data were recorded at  $512 \text{ Mbits s}^{-1}$  and then correlated to produce 8 spectral windows (IFs) each with 8 MHz bandwidth, 32 channels and both circular polarizations (RR, LL). After obtaining a preliminary model for the source, we used it for a run of fringe-fitting in order to better determine delay and rate of the phase variations. After some phase-only self-calibration iterations, we also ran an amplitude self-calibration iteration using a solution interval longer than the scans length (30 min) in order to correct any residual systematic shifts in amplitude. To perform the imaging we used Multi-Scale CLEANing, which is more efficient at modelling extended structures [2, 10].

The final image of MG J0751+2716 at 1.65 GHz can be seen in Fig. 1. The total flux density of this source was measured to be about 350 mJy. The radio morphology is rather complex and in agreement with previous MERLIN imaging, but at 50 times better angular resolution [6]. A new double component is detected for the first time (Fig. 1).

The Keck AO image clearly shows a bright early-type lensing galaxy in the centre, two bright lensed components and a fainter extended arc surrounding the lensing galaxy. Interestingly, the optical emission does not follow the NIR and radio emission, but two bluer compact components are detected in the south-west and north-east parts of the ring with a separation of  $\sim 0.8$  arcsec (Fig. 2). The astrometric alignment between the images was performed by using the lensing galaxy position provided by the lens model.

## 2.3 Herschel observations

MG J0751+2716 was observed with the Herschel SPIRE instrument at 250, 350 and  $500 \mu\text{m}$ . These FIR observations, supplemented with data from the literature, were fitted with an SED consisting of modified black body for the

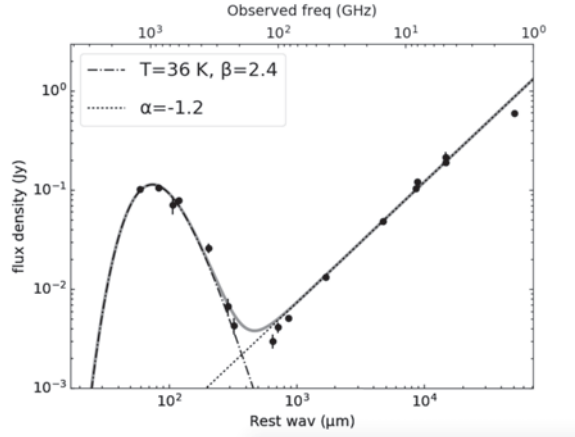


Fig. 3. SED of MG J0751+2716, the data are from Herschel SPIRE, SCUBA, Mambo, PdBI and JVLA. The legend shows the fitted temperature of the heated dust,  $T$ , the index of the Rayleigh-Jeans slope,  $\beta$ , and the spectral index of the synchrotron emission,  $\alpha$

dust emission and a power law for radio synchrotron emission (Fig. 3). We fit for both the temperature of the black body,  $T$ , and the Rayleigh-Jeans slope,  $\beta$ . The fitted dust temperature is  $38.1 \pm 2.3$  K, with a FIR luminosity  $L_{42.4-112.5\mu m} = (2.7 \pm 0.2) \times 10^{13} / \mu L_{\odot}$ . The inferred SFR of  $(5.2 \pm 0.5) \times 10^3 / \mu M_{\odot} \text{ yr}^{-1}$  is too high to be explained with the jet-induced star-formation process alone, even after accounting for the magnification of the dust which was estimated to be 16 [1].

### 3 Lens modelling and pixellated source reconstruction

In order to perform the lens modelling of the multi-wavelength dataset for the gravitationally lensed system MG J0751+2716 we used the fully Bayesian lens modelling technique developed by Vegetti and Koopmans [18]. We modelled the data by using an elliptical power-law mass distribution with an external shear, required because the main lensing galaxy is part of a small group of galaxies. The lens modelling of the EVN dataset was performed in the visibility plane, using the approach of [12]. The important advantage of using the visibility plane instead of the image plane consists of bypassing any possible errors introduced during the deconvolution process, that would alter the intrinsic structure of the radio jets. The source reconstruction of MG J0751+2716 (Fig. 2) consists of two distinct optical components, separated by a projected distance of  $\sim 1$  kpc, that differ strongly in colour. The reddest component is found to be extremely compact, while the blue star-forming object is more diffuse and shows multiple brightness components. We speculate that the two optical-infrared components are likely interacting and, there-

fore, may be the responsible for the star-formation across the system. The radio-jets, which extend in projection over  $\sim 0.5$  kpc, are not apparently interacting with the blue star-forming component. Therefore their role in the SFR within MG J0751+2716 is still unclear.

#### 4 Summary

We have presented new high-angular resolution imaging of the gravitationally lensed radio-loud source MG J0751+2716 at redshift 3.2. By using an advanced gravitational lens modelling procedure, our source reconstruction finds that the morphology of MG J0751+2716 is rather complex. This high redshift source consists of two different optical components, both of them compact and separated by a projected distance of  $\sim 1$  kpc, and extended radio jets, which are hosted by the reddest component of the system. However, in order to test this hypothesis and locate where the star-formation takes place, we are now extending our analysis to the CO(1-0) JVLA data and in the future spatially resolved high excitation gas and heated dust observations. The information about the dynamics of the gas could determine whether the jets are contributing positively to the star-formation in this system.

#### References

1. *Alloin D., Kneib J. P., Guilloteau S., et al.* Dust and molecular content of the lensed quasar, MG0751+2716, at  $z = 3.2$  // *Astron. & Astrophys.* — 2007. — Vol. 470. — P. 53–60.
2. *Conrwell T. J.* Multiscale CLEAN Deconvolution of Radio Synthesis Images // *IEEE Journal of Selected Topics in Signal Processing.* — 2008. — Vol. 2, Is. 5. — P. 793–801.
3. *Hopkins P., Quataert E., Murray N.* Self-regulated star formation in galaxies via momentum input from massive stars // *Monthly Notices of the Royal Astronomical Society.* — 2011. — Vol. 417, Is. 2. — P. 950–973.
4. *Hopkins P., Cox T. J., Hernquist L., et al.* Star formation in galaxy mergers with realistic models of stellar feedback and the interstellar medium // *Monthly Notices of the Royal Astronomical Society.* — 2013. — Vol. 430, Is. 3. — P. 1901–1927.
5. *Lagattuta D., Vegetti S., Fassnacht C. D.* SHARP — I. A high-resolution multiband view of the infrared Einstein ring of JVAS B1938+666 // *Monthly Notices of the Royal Astronomical Society.* — 2012. — Vol. 424, Is. 4. — P. 2800–2810.
6. *Lehár J., Burke B. F., Conner S. R.* The Gravitationally Lensed Radio Source MG 0751+2716 // *Astronomical Journal.* — 1997. — Vol. 114. — P. 48–53.

7. *Madau P., Dickinson M.* Cosmic Star-Formation History // Annual Review of Astronomy and Astrophysics. — 2014. — Vol. 52. — P. 415–486.
8. *Morganti R., Fogasy J., Paragi Z., et al.* Radio Jets Clearing the Way Through a Galaxy: Watching Feedback in Action // Science. — 2013. — Vol. 341, Is. 6150. — P. 1082–1085.
9. *Podigachoski P., Barthel P. D., Haas M., et al.* Star formation in  $z > 1$  3CR host galaxies as seen by Herschel // Astronomy & Astrophysics. — 2015. — Vol. 575. — ID A80. — P. 28.
10. *Rich J. W., de Blok W. J. G., Cornwell T. J.* Multi-Scale CLEAN: A Comparison of its Performance Against Classical CLEAN on Galaxies Using THINGS // The Astronomical Journal. — 2008. — Vol. 136, Is. 6. — P. 2897–2920.
11. *Riechers D. A., Carilli C. L., Maddalena R. J.* CO ( $J = 1 \rightarrow 0$ ) in  $z > 2$  Quasar Host Galaxies: No Evidence for Extended Molecular Gas Reservoirs // The Astrophysical Journal Letters. — 2011. — Vol. 739, Is. 1. — ID. L32. — P. 6.
12. *Rybak M., McKean J. P., Vegetti S., et al.* ALMA imaging of SDP.81 — I. A pixelated reconstruction of the far-infrared continuum emission // Monthly Notices of the Royal Astronomical Society: Letters. — 2015. — Vol. 451, Is. 1. — P. L40–L44.
13. *Rybak M., Vegetti S., McKean J. P., et al.* ALMA imaging of SDP.81 - II. A pixelated reconstruction of the CO emission lines // Monthly Notices of the Royal Astronomical Society: Letters. — 2015. Vol. 453, Is. 1. — P. L26–L30.
14. *Silk J.* Ultraluminous starbursts from supermassive black hole-induced outflows // Monthly Notices of the Royal Astronomical Society. — 2005. — Vol. 364, Is. 4. — P. 1337–1342.
15. *Spingola C., Dallacasa D., Orienti M., et al.* Radio follow-up of the gamma-ray flaring gravitational lens JVAS B0218+357 // Monthly Notices of the Royal Astronomical Society. — 2016. — Vol. 457, Is. 2. — P. 2263–2271.
16. *Timmons N., Cooray A., Riechers D. A., et al.* Multi-wavelength Lens Reconstruction of a Planck and Herschel-detected Star-bursting Galaxy // The Astrophysical Journal. — 2016. — Vol. 829, Is. 1. — ID. 21. — P. 11.
17. *Tonry J. L., Kochanek C. S.* Redshifts of the Gravitational Lenses MG 0414+0534 and MG 0751+2716 // The Astronomical Journal. — 1999. — Vol. 117, Is. 5. — P. 2034–2038.
18. *Vegetti S., Koopmans L. V. E.* Bayesian strong gravitational-lens modelling on adaptive grids: objective detection of mass substructure in Galaxies // Monthly Notices of the Royal Astronomical Society. — 2009. — Vol. 392, Is. 3. — P. 945–963.